



Vulnerability of groundwater resources to nitrate pollution: A simple and effective procedure for delimiting Nitrate Vulnerable Zones



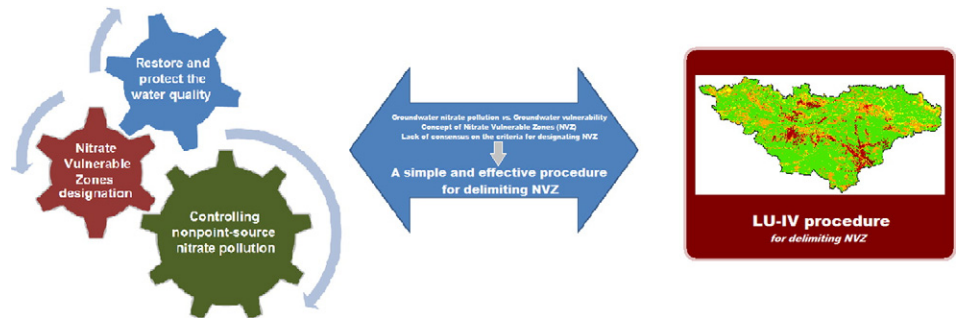
Mercedes Arauzo*

Dpto. de Contaminación Ambiental, Instituto de Ciencias Agrarias ICA-CSIC, Serrano 115 dpdo., 28006 Madrid, Spain

HIGHLIGHTS

- A simple and effective procedure (LU-IV) was developed for delimiting the NVZ.
- LU-IV procedure combines intrinsic vulnerability and risks associated with land use.
- 100% of the alluvial aquifers were affected by or at risk from nitrate pollution.
- High to extreme vulnerability to NO₃-pollution was found in 7% of the territory.
- The current officially designated NVZ should be extended from 328 to 1728 km².

GRAPHICAL ABSTRACT



ARTICLE INFO

Article history:

Received 19 May 2016

Received in revised form 15 September 2016

Accepted 16 September 2016

Available online 1 October 2016

Editor: D. Barcelo

Keywords:

Diffuse pollution

Hydrogeological factors

Land use

Nitrates Directive

ABSTRACT

This research was undertaken to further our understanding of the factors involved in nonpoint-source nitrate pollution of groundwater. The shortcomings of some of the most commonly used methods for assessing groundwater vulnerability have been analysed and a new procedure that incorporates key improvements has been proposed. The new approach (LU-IV procedure) allows us to assess and map groundwater vulnerability to nitrate pollution and to accurately delimit the Nitrate Vulnerable Zones. The LU-IV procedure proved more accurate than the most widely used methods to assess groundwater vulnerability (DRASTIC, GOD), when compared with nitrate distribution in the groundwater of 46 aquifers included in the study (using the drainage basin as the unit of analysis). The proposed procedure stands out by meeting the following requirements: (1) it uses readily available parameters that provide enough data to feed the model, (2) it excludes redundant parameters, (3) it avoids the need to assign insufficiently contrasted weights to parameters, (4) it assesses the whole catchment area that potentially drains N-polluted waters into the receptor aquifer, (5) it can be implemented within a GIS, and (6) it provides a multi-scale representation.

As the LU-IV procedure has been demonstrated to be a reliable tool for delimiting NVZ, it could be particularly interesting to use it in countries where certain types of environmental data are either not available or have only limited availability.

Based on this study (and according to the LU-IV procedure), it was concluded that an area of at least 1728 km² should be considered as NVZ. This sharply contrasts with the current 328 km² officially designated in the study area by the Spain's regional administrations. These results highlight the need to redefine the current NVZ designation, which is essential for an appropriate implementation of action programmes designed to restore water quality in line with Directive 91/676/EEC.

© 2016 Elsevier B.V. All rights reserved.

* Dpto. de Contaminación Ambiental, Instituto de Ciencias Agrarias ICA-CSIC, Serrano 115 dpdo., 28006 Madrid, Spain.
E-mail address: mercedes.arauzo@csic.es.

1. Introduction

What do we really understand by “Nitrate Vulnerable Zones”? According to the Nitrates Directive of the European Union (91/676/EEC; Council of the European Communities, 1991) Nitrate Vulnerable Zones (NVZ) are areas of land that drain into waters affected by nitrate pollution. Nitrate from nonpoint sources has been identified as the main cause of groundwater degradation in Europe (Sutton et al., 2011). Of these nonpoint sources, nitrogen fertilization represents the most important input of nitrate into groundwater and may cause a significant change in groundwater geochemistry (Menció et al., 2016). Farmers in designated NVZ are therefore required to comply with measures laid out in action programmes designed to restore water quality.

The Nitrates Directive establishes that both surface freshwater and groundwater should be considered affected by nitrate pollution when their nitrate contents exceed 50 mg L^{-1} . Nitrate levels above this threshold are considered dangerous to human health and to the environment (Sutton et al., 2011). Within the range of $25\text{--}50 \text{ mg L}^{-1}$ of nitrate, water can be considered at risk of becoming polluted if no protective measures are taken (European Commission, 2000).

Although the EU has made significant efforts to reduce nitrate pollution, there are still important discrepancies in the way that NVZ are designated in different European regions and countries (European Commission, 2010). In fact, recent studies have shown that inadequate designations of NVZ can lead to unsatisfactory results in attempts to reduce water pollution caused by nitrate (Arauzo and Martínez-Bastida, 2015; Arauzo et al., 2011; Worrall et al., 2009).

One major obstacle to a more efficient implementation of EU environmental policies for nitrate pollution control is the lack of consensus on the criteria to be used for designating NVZ (De Clercq et al., 2001). To address this complex issue, it is first necessary to examine the elusive concept of groundwater vulnerability. It is usually defined as “the sensitivity of an aquifer to being adversely affected by an imposed contaminant load” or “the intrinsic susceptibility of an aquifer to contamination” (Witkowski et al., 2007). Two different types of groundwater vulnerability assessment are generally considered: intrinsic and specific assessments. Intrinsic vulnerability is based on an assessment of natural climatic, geological and hydrogeological attributes, whereas specific vulnerability is mainly assessed in terms of the risk of the groundwater system becoming exposed to contaminant loading (Witkowski et al., 2007). In the case at hand, assessing specific groundwater vulnerability to nitrate pollution involves analysing the risk of exposure to N-compounds in areas where there is a considerable degree of intrinsic vulnerability.

Foster (2007) asserted that “there is little doubt that the concept of aquifer vulnerability (and its practical manifestation in land surface mapping) is a valuable tool for groundwater quality protection”. Even so, no consensus has yet been reached as to which environmental factors must be considered in assessments of groundwater vulnerability. Aquifer recharge, aquifer media, topography, soil properties, hydraulic conductivity, the lithology of the overlying strata, groundwater hydraulic confinement and the depth to the water table, all tend to be key attributes for both intrinsic and specific vulnerability. Several authors have also considered groundwater flow, the travel time of the contaminant and local land use in assessments of groundwater vulnerability (Witkowski et al., 2007). On the basis of these parameters, a variety of groundwater vulnerability indexes have been proposed in recent decades (Aller et al., 1987; Anjali et al., 2015; Dixon, 2005; Foster, 1987; Huan et al., 2012; Lubianetzky et al., 2015; Martínez-Bastida et al., 2010; Neshat and Pradhan, 2015; Secunda et al., 1998; Witkowski et al., 2007; Wachniew et al., 2016). Of these, the DRASTIC index (Aller et al., 1987) and the GOD index (Foster, 1987; Foster et al., 2002) have been the most widely used to assess intrinsic groundwater vulnerability.

The DRASTIC model uses seven media parameters (depth to the water table, aquifer recharge, aquifer media, soil media, topography, impact of vadose zone and hydraulic conductivity) in an additive formulation. These parameters are weighted according to their relative importance to the pollution potential. The GOD model incorporates three parameters

(groundwater confinement, overlying strata and depth to groundwater) into a multiplicative algorithm. Martínez-Bastida et al. (2010) observed a great similarity between intrinsic vulnerability maps obtained using both the DRASTIC and GOD approaches, underlining the simplicity of the latter. The same authors also suggested that the ratings that DRASTIC assigns to the hydraulic conductivity parameter (which increase with the velocity of the groundwater flow) reflect the ability of the system to transport the pollutant through the saturated zone, but do not assess its vulnerability. Moreover, Hamza et al. (2015) demonstrated that all the DRASTIC parameters are equally significant irrespective of their assigned weights. Stigter et al. (2006) suggested two additional weaknesses of the DRASTIC model: the excessive emphasis on the attenuation capacity of the unsaturated zone and the difficulty of obtaining accurate estimates of aquifer recharge and hydraulic conductivity. With regard to the GOD index, Arauzo (2014) pointed out that the model only provides information about the area above the aquifer and not about the entire aquifer catchment area (given that its G and D parameters are assigned a zero value in areas where there is no groundwater). This imposes a limitation for sloped areas in which advective N-transport can take place in the vadose zone by subsurface runoff, until the water reaches the aquifer.

Debernardi et al. (2012), Holman et al. (2005) and Stigter et al. (2006) all expressed doubts about the reliability of estimations of groundwater vulnerability because of the discrepancies that were sometimes observed between vulnerability maps and nitrate pollution maps. However, Arauzo and Martínez-Bastida (2015) suggested that such discrepancies can be adequately explained by considering advective N-transport and accumulation/dilution processes in the saturated zone and/or N-transport by subsurface runoff in the vadose zone. They highlighted the importance of distinguishing between the NVZ (areas of the catchment area of an aquifer from which N-leaching occurs) and the zones of the aquifer in which groundwater is polluted by nitrate. Unfortunately, on many occasions these two concepts have been mistakenly taken as interchangeable in scientific and technical literature and this has sometimes adversely affected NVZ designations.

In short, the assessment of groundwater vulnerability to nitrate pollution and the delimiting of NVZ could be improved by: (1) using parameters that provide enough useful data to feed the model, (2) eliminating redundant parameters, (3) eliminating the assignment of insufficiently contrasted weights to parameters, and (4) assessing the entire catchment area that could potentially drain waters polluted by nitrate into the receptor aquifer. It should also be implementable in a geographic information system (GIS) and provide a multi-scale representation (ranging from the local to the regional scale).

The primary aim of this study was, therefore, to develop a new method for assessing and mapping groundwater vulnerability to nitrate pollution that meets the above-mentioned requirements. The proposed method includes two steps: (1) applying a new algorithm that improves the assessment and mapping of intrinsic groundwater vulnerability and (2) incorporating a new procedure, based on logical evaluation, for assessing and mapping the specific groundwater vulnerability to nitrate pollution.

The present investigation also sought to further our understanding of the factors involved in the nonpoint-source nitrate pollution of groundwater resources. This was conducted through a joint analysis of groundwater nitrate distribution in a diverse range of aquifers and the NVZ (delineated by the aforementioned method) potentially draining into them. The study area (the upper River Ebro basin, north of Spain) presents great variety in terms of its geology, topography, hydrology, weather conditions and land use. More specifically, the following objectives were established: (1) to model the spatial distribution of nitrate content in the 46 main aquifers of the upper River Ebro basin on an aquifer by aquifer basis, (2) to analyse the relationship between groundwater nitrate distribution, water table elevation and flow direction, (3) to develop a methodology for assessing and mapping intrinsic groundwater vulnerability (the new IV index) and specific groundwater vulnerability to nitrate pollution (the new LU-IV procedure) in a way that improves previous approaches, (4) to generate thematic maps of intrinsic and specific

groundwater vulnerability, (5) to validate the proposed method and to compare this with the DRASTIC and GOD methods, and (6) to define the NVZ according to the selected approach and to compare the results with the officially designed NVZ in the study area until now.

2. Study area

The study area comprises 21 river basins that drain into the River Ebro (upper River Ebro basin; north of Spain), covering a total area of 25,664 km². There are 46 groundwater bodies below the upper River Ebro basin (Fig. 1), occupying 18,704 km². The majority of these groundwater bodies include one major aquifer and various other minor ones (MAGRAMA, 2005). In this research, we have studied the 46 major aquifers, which together present a wide variety of properties, types and sizes (Table 1).

The climate in the study area is continental-Mediterranean, with mean annual precipitations ranging from 360 to 1530 mm (Botey et al., 2013), depending on the altitude, which ranges from 260 to 2884 m above sea level. This topographically and geologically complex territory has a variety of land uses (MARM, 2009; Fig. 2), some of which are major anthropogenic sources of N-inputs.

The implementation of the EU Nitrates Directive in Spain is the responsibility of the regional administrations. The study area includes territories that form part of six different regional administrations: Castilla y León, Cantabria, Aragón, La Rioja, País Vasco and Navarra. To date, La Rioja, País Vasco and Navarra have officially designated a total of eight NVZ within the study area (Fig. 1), jointly covering an area of 328 km² (1.3% of the study area).

3. Material and methods

3.1. Nitrate in groundwater

The map of the nitrate levels in groundwater was drawn up using data on nitrate concentrations for 872 sampling points distributed over the 46 main aquifers in the study area. These were mainly irrigation wells, but also included boreholes and springs. The average nitrate concentrations over a period of five hydrological years (from October 2005 to September 2010) were used to create the map.

Spatial modelling of groundwater nitrate concentration was performed, aquifer by aquifer, applying the Spline Interpolation tool (Spatial Analyst Tools in ArcGIS 10; ESRI, 2011) to the shapefiles of sampling points. The resulting 46 raster maps were then merged (using Mosaic to New Raster) to obtain a map of the nitrate levels in groundwater for the study area.

The Ebro Hydrographic Confederation (Confederación Hidrográfica del Ebro), the Geological and Mining Institute of Spain (Instituto Geológico y Minero de España) and the Basque Water Agency (Agencia Vasca del Agua) provided the hydrochemical information.

3.2. Water table elevation

Water table elevation determines the flow direction of groundwater and therefore that of the advective transport of solutes within the saturated zone. The map of water table elevation was generated from measurements of the depth to the water table at 1042 sampling points (irrigation wells and boreholes). As for the map of nitrate concentration, we used average values for the depth of the water table from October 2005 to September 2010.

Shapefiles of points of water table elevation were generated, aquifer by aquifer, by subtracting the depth to the water table from the corresponding ground surface elevation at each sampling point. This was done using a digital elevation model (DEM) with a resolution of 10 m. Individual raster maps of water table elevation were then obtained from the shapefiles of points, using the Spline Interpolation.

The Ebro Hydrographic Confederation supplied the information about the sampling points.

Pearson's correlation coefficient was used to analyse the relationship between the raster of water table elevation and the raster of nitrate concentration in groundwater on an aquifer by aquifer basis. The aim was to explore the role of the advective transport of nitrate within the saturated zone in the distribution of nitrate in groundwater. Correlations were carried out using Band Collection Statistics (Spatial Analyst Tools).

3.3. Groundwater vulnerability

In this study, a two-step GIS-based method was developed in order to satisfy the requirements outlined in the Introduction for improving

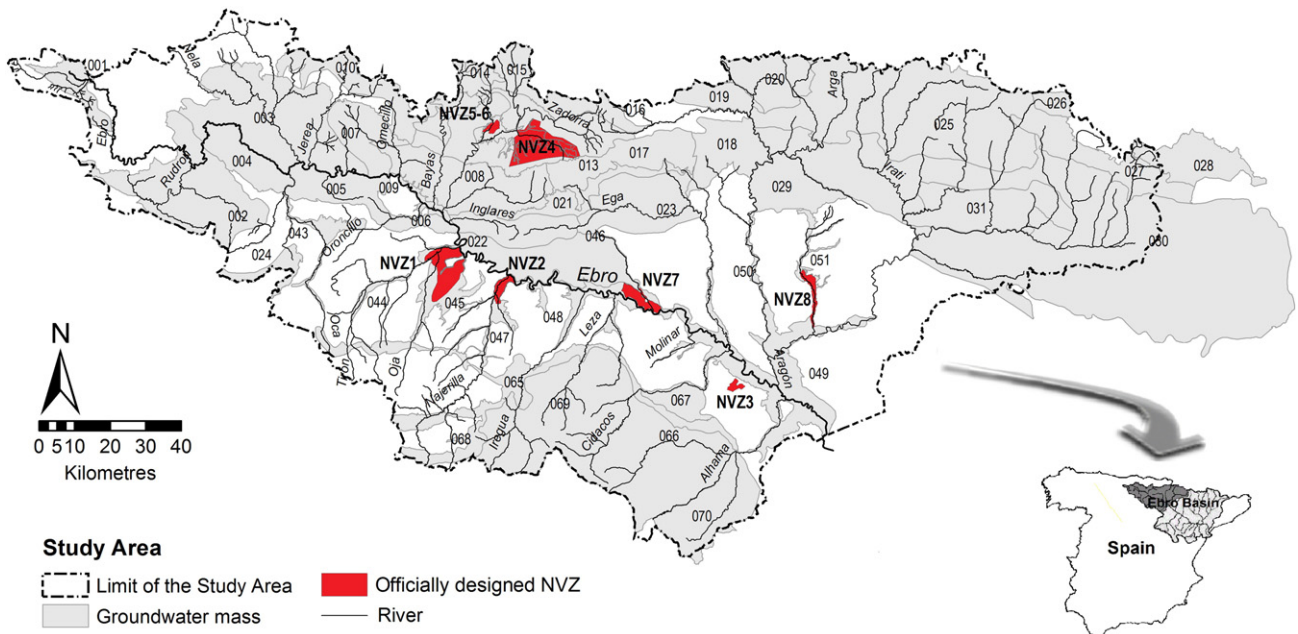


Fig. 1. Upper River Ebro basin (northern Spain); the 46 groundwater bodies (identified by the CHE-code) and the eight Nitrate Vulnerable Zones (NVZ) officially designated within the study area are shown (CHE, 2015).

Table 1
Characteristics of the 46 major aquifers in the study area.

Groundwater body (CHE-code ^a)	Area (km ²)	Thickness (m)	Type	Dominant geology
Fontibre (001)	150	300–750	Unconfined	Limestone and Jurassic dolomite
Páramo de Sérano y Lora (002)	744	40–200	Unconfined	Cretaceous limestone
Sinclinal de Villarcayo (003)	879	150–400	Unconfined	Cretaceous limestone
Manzanedo-Oña (004)	232	200–400		Limestone and Cretaceous dolomite
Montes Obarenes (005)	270	250	Unconfined	Limestone and Cretaceous dolomite
Pancorbo-Conchas de Haro (006)	73			Upper Cretaceous Series
Valderejo-Sobrón (007)	251			Cretaceous limestone
Sinclinal de Treviño (008)	579	300	Unconfined	Paleocene limestone
Aluvial de Miranda de Ebro (009)	47		Unconfined	Alluvial deposits
Calizas de Losa (010)	291			Limestone
Calizas de Subijana (011)	195		Unconfined	Limestone
Aluvial de Vitoria (012)	108	1–11	Unconfined	Alluvial deposits
Cuartango-Salvaterra (013)	594		Unconfined	Limestone
Gorbea (014)	34			Carbonate formations
Altube-Urkilla (015)	273			Reef limestone, calcarenite and breccias
Sierra de Aizkorri (016)	61			Reef limestone
Sierra de Urbasa (017)	358	300	Unconfined	Limestone and dolomite
Sierra de Andía (018)	300		Semi-confined	Limestone and Paleocene dolomite
Sierra de Aralar (019)	140	200–1000	Semi-confined	Reef limestone
Basaburua-Ulzama (020)	285	100–500		Carbonate formations
Izki-Zudaire (021)	158		Unconfined	Sandstone and calcareous sandstones
Sierra de Cantabria (022)	252			Tertiary conglomerates and limestones
Sierra de Lóquiz (023)	448		Unconfined	Upper Cretaceous limestone
Bureba (024)	84	450		Carbonate formations
Alto Arga-Alto Irati (025)	1580	100–220	Unconfined	Limestone and dolomite
Larra (026)	63	400	Unconfined	Cretaceous limestone
Ezcaurre-Peña Telera (027)	376	100–250		Carbonate formations
Alto Gállego (028)	296			Fissured granite and karstic limestone
Sierra de Alaiz (029)	279			Sandstone, conglomerates, carbonate formations
Sinclinal de Jaca-Pamplona (030)	4066		Confined	Calcareous breccias
Sierra de Leyre (031)	491		Unconfined	Limestone
Aluvial del Oca (043)	92		Unconfined	Alluvial deposits
Aluvial del Tirón (044)	30		Unconfined	Alluvial deposits
Aluvial del Oja (045)	213		Unconfined	Alluvial deposits
Laguardia (046)	473		Unconfined	Miocene sandstones
Aluvial de Najerilla-Ebro (047)	117		Unconfined	Alluvial deposits
Aluvial de La Rioja-Mendavia (048)	188		Unconfined	Alluvial deposits
Aluvial Ebro-Aragón: Lodosa-Tudela (049)	643		Unconfined	Alluvial deposits
Aluvial del Arga Medio (050)	30	10–15	Unconfined	Alluvial deposits
Aluvial del Cidacos (051)	61	20	Unconfined	Alluvial deposits
Prodluengo-Anguiano (065)	248	40–200		Carniolas, dolomite and limestone
Fitero-Arnedillo (066)	97			Carbonate formations and Cretaceous limestone
Detrítico de Arnedo (067)	124			Conglomerates, sands, Quaternary glaci
Mansilla-Neila (068)	199	40–50	Unconfined	Limestone and calcarenite
Cameros (069)	1814	80–1100	Unconfined	Conglomerates, sandstones, limonites, sandy limestone, marl and gypsum
Añavieja-Valdegutur (070)	416	340–1000	Unconfined	Conglomerates, loam sandy limestone

^a CHE-code assigned by CHE (2015).

the assessment and mapping of groundwater vulnerability to nitrate pollution. This novel approach implies the use of a geospatial predictive model that allows the mapping of intrinsic groundwater vulnerability (Step 1) and specific groundwater vulnerability to nitrate pollution (Step 2). Step 1 employs a new algorithm designed to assess intrinsic vulnerability (the IV index) which is based on robust data. Step 2 develops a new procedure designed to assess specific vulnerability to nitrate pollution (the LU-IV procedure). The LU-IV procedure combines a map of intrinsic vulnerability (based on the IV index) with an assessment of the risks associated with different land uses (using the Over tool from the Math > Logical toolset of Spatial Analyst Tools).

3.3.1. Step 1: intrinsic groundwater vulnerability

3.3.1.1. *The IV index: a simple algorithm.* The IV index for assessing the intrinsic vulnerability of groundwater was developed from the mean equation:

$$IV = \frac{\sum_{j=1}^n Pr_j}{n} \quad (1)$$

where Pr is the rating of each environmental parameter and j represents the n compositional parameters that make up the index.

The most basic formulation of the new IV index was based on four environmental parameters that are commonly related to intrinsic groundwater vulnerability and that provide enough data to generate an accurate map, as follows:

$$IV = \frac{L + D + T + P}{4} \quad (2)$$

where L is the rating of the risks associated with the lithology of the vadose zone, D is the rating of the risks associated with the depth of the water table, T is the rating of the risks associated with topography (percentage of slope) and P is the rating of the risks associated with average annual precipitation (Table 2). The ratings applied to ranges of these parameters were based on those proposed by Aller et al. (1987) for the DRASTIC index and by Foster et al. (2002) for the GOD index. This formula does not pre-assign different weights for the different parameters to avoid using insufficiently contrasted values (Hamza et al., 2015). The flexibility of the model makes it possible to include additional parameters related to intrinsic groundwater vulnerability, if available. In other

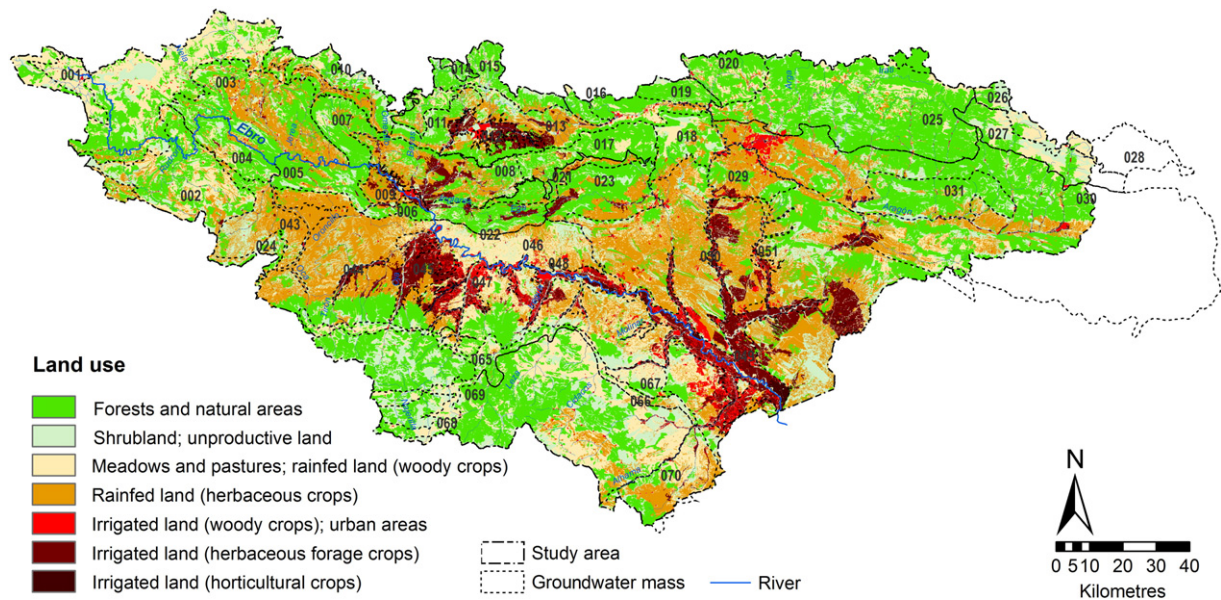


Fig. 2. Land use in the study area (extracted from MARM, 2009).

words, it would have been desirable to have had data on the risks associated with soil permeability (Aller et al., 1987) and to have included this in the index; unfortunately, no soil maps were available for the study area at the required scale of 1:50,000.

For ease of interpretation, a single scale (ranging from 1 to 10) was used for the IV index and also for the parameters comprising it. The different risks were grouped into five categories: negligible risk: 1–2; low risk: 3–4; moderate risk: 5–6; high risk: 7–8; extreme risk: 9–10. These categories were defined according to the linear regression between the nitrate and IV index datasets (nitrate levels above 50 mg L^{-1} were related to IV values from 7 to 10).

The map of intrinsic groundwater vulnerability based on the IV index was created from the thematic rasters of parameters L , D , T and P , using the Raster Calculator (Spatial Analyst Tools) to run the Eq. (2). It should be noted that, unlike in the DRASTIC and GOD models, the rasters L , D , T and P covered the entire catchment areas that potentially drained into the aquifers and not only the land surfaces above them.

Parameters L , D , T and P are described below.

3.3.1.2. Risks associated with the lithology of the vadose zone (L). The vadose zone controls the penetration and downward movement of recharge, confines pollutants, and determines the time taken for contaminants to reach the aquifer. The lithological character and degree of consolidation of the vadose zone determine the contaminant attenuation capacity (Foster et al., 2002).

For mapping the risks associated with the lithology of the vadose zone (L) we used the digital version of the Geologic map of Spain at a scale of 1:50,000 (MAGNA Series, produced by the Spanish Geological Institute; CHE, 2015). Ratings applied to ranges of lithological types (Table 2) were assigned according to Foster et al. (2002), but transformed to a scale ranging from 1 to 10. The ratings were added to the attribute table of the geologic map. We then used Polygon to Raster to obtain the raster map of L .

3.3.1.3. Risks associated with the depth of the water table (D). The depth of the water table determines the time taken for water-soluble contaminants to travel from the land surface down to the aquifer (Aller et al., 1987; Foster et al., 2002). Aquifers close to the surface are therefore likely to be contaminated faster than deeper ones.

The minimum value of the depth to the water table (registered at each sampling point) over the period from October 2005 to September 2010 was used in the calculations. The criterion of “minimum depth”

offered the least favourable scenario, in which the water table was nearest the surface. Shapefiles of points of the depth to the water table were used to generate their respective rasters (aquifer by aquifer) using the Spline Interpolation tool. The resulting rasters were reclassified according to the ranges and ratings presented in Table 2 (based on Foster et al., 2002) and merged (using Mosaic to New Raster) to generate the raster map of D .

3.3.1.4. Risks associated with topography (T). Topography helps control the likelihood that a pollutant will run off or remain on the surface in one area long enough to infiltrate (Aller et al., 1987). Areas that are relatively flat are considered to be more susceptible to infiltration. As such, they may be more vulnerable to leaching losses than other, steeper areas.

A raster map of topographic slope was generated from a DEM with a resolution of 10 m, using Slope (Spatial Analyst Tools). To create the raster of the risks associated with topography (T) ratings for the slope ranges (according to Aller et al., 1987; Table 2) were assigned using Reclassify (Spatial Analyst Tools).

3.3.1.5. Risks associated with annual precipitation (P). Lubianetzky et al. (2015), Martínez-Bastida et al. (2010) and Stigter et al. (2006) have pointed out the difficulty of obtaining enough reliable estimates for certain key parameters, such as aquifer recharge, to assess groundwater vulnerability. Many of the factors that affect aquifer vulnerability within the context of recharge availability (soil media, evapotranspiration, topography, infiltration, vegetative cover, runoff, precipitation, freeze/thaw conditions, soil permeability and porosity) also influence vulnerability factors related to the overlying unsaturated zone (Lubianetzky et al., 2015). On the other hand, data relating to several of these factors are often unavailable in the quantity and quality needed to properly feed the model – e.g., the reference evapotranspiration (ET₀); the parameter provided by the weather stations) differs greatly from the real evapotranspiration. This is largely because the ground cover, canopy properties and aerodynamic resistance of the vegetative cover differ from those associated with the reference grass at the weather stations (Allen et al., 1998; Arauzo et al., 2010). However, such improper uses of ET₀ to estimate water balances and aquifer recharges (instead of real evapotranspiration) can often be found in studies and reports conducted at both the regional and river basin scales.

Bearing all of this in mind, the amount of precipitation (in the form of annual precipitation) was explored as an indicator of aquifer

recharge. This information is easily obtainable and cannot be confused with overlying unsaturated zone factors. The average intensity of precipitation (annual precipitation divided by the number of rainy days per year; Lubianetzky et al., 2015) was not used due to the uneven pattern of the rainfall in the study area (Botey et al., 2013).

It also could be argued that irrigation agriculture strongly contributes to aquifer recharge. However, this risk factor (which is associated with land use) will be specifically addressed in Step 2.

Average monthly precipitation from 1981 to 2010 for 492 weather stations distributed across the River Ebro basin was obtained from the network of the Spanish Meteorological Agency (Botey et al., 2013). These data were used to create a shapefile of points with the average annual precipitation from 1981 to 2010, from which a raster map was generated using Interpolation (Spatial Analyst Tools).

The map of the risks associated with annual precipitation (P) was created from the raster of the average annual precipitation. Ratings applied to precipitation ranges (Table 2) were assigned using Reclassify. These ratings were based on the results of a research project that monitored precipitation and drainage in agricultural soils in the study area on an hourly basis, from 2007 to 2010 (Arauzo and Valladolid, 2013).

3.3.1.6. Sensitivity analysis. Single-parameter sensitivity analyses were performed to compare the theoretical weights assigned to the vulnerability parameters and their effective counterparts. These effective weights are influenced by the weight assigned to each individual parameter and the value of a single parameter (Javadi et al., 2011). We used the following equation:

$$W = \left(\frac{Pr * Pw}{V} \right) * 100 \quad (3)$$

where W is the effective weight of each parameter, Pr and Pw are the rating and theoretical weight assigned to each parameter, respectively, and V is the value of the vulnerability index (Babiker et al., 2005).

For the IV index (Eq. (2)) the value of Pw is equal to $\frac{1}{4}$ for every individual parameter. Single-parameter sensitivity analyses were performed, grid by grid, using Raster Calculator.

As the weighting systems used to generate the vulnerability index are area dependent (Babiker et al., 2005), it would be reasonable to expect differences in effective weights to vary from one area to another. To assess and compare these variabilities, sensitivity analyses were performed for the entire study area and also for the 21 individual river basins in the study area.

3.3.2. Step 2: specific groundwater vulnerability

3.3.2.1. The LU-IV procedure. The LU-IV procedure was developed as a tool for assessing and mapping groundwater vulnerability to nitrate pollution and delimiting the NVZ. This new procedure combines the intrinsic vulnerability map (based on the IV index: Step 1) and the map of the risks associated with land use, using the Over tool (from the Math > Logical toolset).

To create the map of risks associated with land use, we used the digital version of the Crops and Land Use map of Spain 2000–2009 (MARM, 2009; Fig. 2) at a scale of 1:50,000. Ranges were established (by grouping land uses according to their respective potentials as sources of nitrate pollution) and ratings were applied to these ranges (Table 2). The ranges and ratings were established in line with the methods described by Secunda et al. (1998), with minor modifications (i.e., the rating applied to rainfed land was increased from 4 to 6, based on the results of research into drainage and N-leaching in agricultural soils in the study area; Arauzo and Valladolid, 2013).

The LU-IV procedure firstly involved reclassifying the original cell values of the raster of intrinsic vulnerability into values of “1” and “0”. The value “1” represented “non-vulnerable areas” (cell values ranging

Table 2

Ranges and ratings for risks associated with environmental parameters related to groundwater vulnerability to nitrate pollution; the scales of the original ratings (in brackets) were transformed to a single scale ranging from 1 to 10.

Risks associated with environmental parameters	
Lithology of the vadose zone (L^a)	
Range	Rating
Calcretes, karst limestones (1.0)	10
Chalky limestones calcarenites (0.9)	9
Alluvial-fan gravels; recent volcanic lavas (0.8)	8
Alluvial and fluvio-glacial sands; sandstones (0.7)	7
Aeolian sands; siltstones, volcanic tuffs; igneous/metamorphic formations and older volcanic formations (0.6)	5
Alluvial silts, loess, glacial till; mudstones, shales (0.5)	3
Residual soils (0.4)	1
Depth to the water table (D^a)	
Range (m)	Rating
All depths (for calcretes, karst limestones, chalky limestones calcarenites, recent volcanic lavas; 1.0)	10
0–5 (0.9)	9
>5–10 (0.8)	8
>10–20 (0.8)	6
>20–50 (0.7)	4
>50 (0.6)	2
None (0.0)	1
Annual precipitation (P^b)	
Range (mm)	Rating
>900	10
>800–900	9
>700–800	8
>600–700	7
>500–600	6
>400–500	5
>300–400	4
>200–300	3
>100–200	2
0–100	1
Topography (T^c)	
Range (% of slope)	Rating
0–2 (10)	10
2–6 (9)	9
6–12 (5)	5
12–18 (3)	3
>18 (1)	1
Land use (LU^d)	
Range	Rating
Irrigated land (horticultural crops; 10)	10
Irrigated land (herbaceous forage crops; 8)	9
Urban areas (5–7)	7
Irrigated land (woody crops; 7)	7
Rainfed land (herbaceous crops; 4)	6
Rainfed land (woody crops; 5)	5
Meadows and pastures (5)	5
Shrubland; unproductive land (1–5)	3
Forests and natural areas (1)	1

^a Source: Foster et al. (2002; original ratings in brackets);

^b Ratings based on hourly measurements of precipitation and drainage from six monitoring stations used in the study area over 40 consecutive months (Arauzo and Valladolid, 2013);

^c Source: Aller et al. (1987; original ratings in brackets);

^d Source: Secunda et al. (1998; original ratings in brackets).

from 1 to 4, with negligible to low intrinsic vulnerabilities) and the value “0” represented “vulnerable areas” (cell values ranging from 5 to 10, with moderate to extreme intrinsic vulnerabilities). The previously obtained raster (intrinsic vulnerability 1–0) was used as the first entry in the Over tool, while the raster of risks associated with land use was used as the second entry in the Over tool. When the Over operation is performed, for cell values in the first input that are equal to “1” the output value will be that of the first input (= 1; in other words, it represents the areas in which land use restrictions do not have to be applied). But where the cell values in the first input correspond to “0”, the output will be that of the second input raster (showing the original

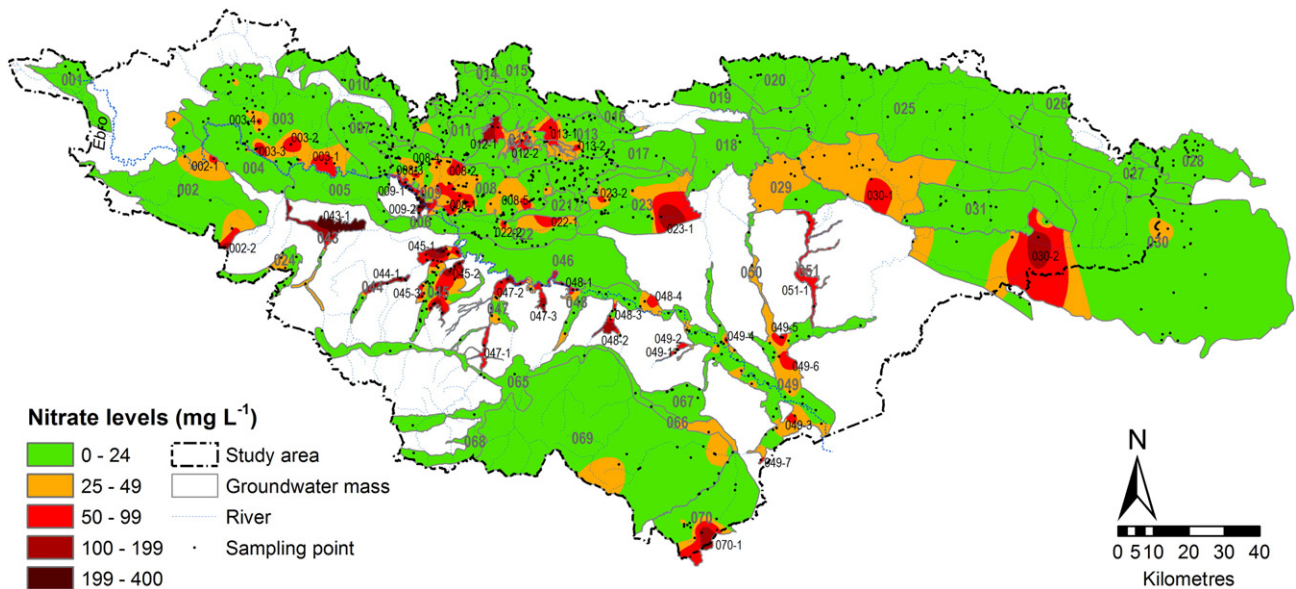


Fig. 3. Nitrate levels in groundwater of the 46 aquifers included in the study; sampling points used for interpolations are shown; polluted groundwater zones ($[\text{NO}_3^-] \geq 50 \text{ mg L}^{-1}$) are labelled using the CHE-code of the aquifer plus a number.

values of the raster of risks associated with land use). Using this procedure, we obtained a map of groundwater vulnerability to nitrate pollution associated with land use. From this, it was then possible to draw polygons delimiting the NVZ using Conversion Tools (ArcGIS 10; ESRI, 2011).

3.3.2.2. Validation of results. Nitrate concentrations in groundwater are generally low under natural conditions and its abundance suggests susceptibility to pollution (Shirazi et al., 2012). For this reason, this indicator has been widely used by many researchers for the validation of groundwater vulnerability models (Boy-Roura et al., 2013; Kura et al., 2015; Martínez-Bastida et al., 2010).

As a first approach to analyse relationships between nitrate distribution in groundwater and different models of groundwater vulnerability, a correlation matrix was generated (using the Band Collection Statistics tool) which included the following thematic rasters: nitrate concentration in groundwater, intrinsic vulnerability based on the GOD index (Arauzo, 2014), intrinsic vulnerability based on the DRASTIC index (a reduced version of DRASTIC; IGME, 2009a, 2009b), intrinsic vulnerability based on the IV index and specific vulnerability to nitrate pollution based on the LU-IV procedure. The objective was to compare the effectiveness of the four models of groundwater vulnerability.

Reality, however, is more complex. As mentioned in the Introduction, certain discrepancies should be expected between vulnerability maps and nitrate pollution maps, most of which can be explained by considering advective N-transport through the vadose and saturated zones. The hydrological dynamics of the drainage basin affects nitrate distribution in groundwater at different levels: nitrate is leached from the surface of the NVZ in the basin as a consequence of excess precipitation or irrigation; before reaching the aquifer, nitrate follows vertical pathways through the vadose zone, but it can also be transported through the basin by subsurface runoff (in areas with slopes); once nitrate has reached the aquifer, groundwater flow paths determine where it is accumulated. Bearing this in mind, a more realistic comparison between the four previously mentioned vulnerability models was performed using the drainage basin as the natural unit of analysis. To compare the four vulnerability criteria, Pearson's correlations were performed between the relative areas corresponding to polluted groundwater and the relative areas of NVZ (as percentages of the total area in each basin) in the 21 drainage basins of the study area, for each of the four models. It was hypothesised that a direct proportionality could be

expected between the relative area of groundwater polluted by nitrate and the relative area of NVZ in a given drainage basin.

3.4. Statistical analysis

The Band Collection Statistics tool (Spatial Analyst Tools) was used to calculate the Pearson's correlation coefficients between pairs of raster datasets. This tool was also used to create a correlation matrix of several thematic rasters. This was done after clipping and resampling the rasters so that they had the same geographic extent and pixel resolution as the one with the smallest extension and lowest resolution.

The Pearson correlation assumes a normal distribution of data and linearity between the two variables. The first task was therefore to check whether these assumptions of normality and linearity had been violated or not. The Normal QQ Plot and General QQ Plot tools (Geostatistical Analyst Tools in ArcGIS 10; ESRI, 2011) were respectively used to do this. Spearman rank correlations were used in cases in which any of the conditions were not satisfied (IBM SPSS Statistics 23.0; IBM Corp., 2014).

4. Results and discussion

4.1. Nitrate distribution in groundwater

The spatial modelling of nitrate concentrations in the 46 aquifers under study (Fig. 3) revealed that 44 zones were polluted by nitrate ($[\text{NO}_3^-] \geq 50 \text{ mg L}^{-1}$) in 17 aquifers; nine of these were alluvial aquifers, six carbonate aquifers and two detrital sedimentary aquifers (Table 1). Another five aquifers showed only areas at risk of being affected by pollution ($[\text{NO}_3^-] \geq 25\text{--}49 \text{ mg L}^{-1}$); one of these was an alluvial aquifer, while the others were detrital sedimentary aquifers. The remaining 24 carbonate aquifers showed low to moderate nitrate concentrations ($[\text{NO}_3^-] < 25 \text{ mg L}^{-1}$).

Alluvial aquifers exhibited the worst conditions: 90% were affected and 10% were at risk of being affected by nitrate pollution. Furthermore, 70% exhibited nitrate contents above 50 mg L^{-1} in 50% to 100% of their total area (Table 3). The carbonate and detrital sedimentary aquifers exhibited somewhat better behaviour: 22% were affected and 11% were at risk of being affected by nitrate pollution; zones with over 50 mg L^{-1} of nitrate represented from 1% to 6% of the total area (Table 3).

Table 3
Maximum nitrate concentrations in the aquifers of the study area (from average values from 2005 to 2010 at each of the sampling points); percentages of affected area ($[\text{NO}_3^-] \geq 50 \text{ mg L}^{-1}$) and area at risk ($[\text{NO}_3^-] \geq 25\text{--}49 \text{ mg L}^{-1}$) relative to the total area of the aquifer; Pearson's correlation (r) between the raster of nitrate concentration and the raster of water table elevation (only for the aquifers affected by and at risk of being affected by nitrate pollution).

Groundwater body (CHE-code)	Max. $[\text{NO}_3^-]$ (mg L^{-1})	Affected area (%)	Area at risk (%)	r	p-Value
001	4	0	0		
002	147	3	20	−0.11	0.003
003	110	7	16	−0.34	0.00001
004	29	0	0		
005	11	0	0		
006	6	0	0		
007	34	0	0		
008	94	13	37	−0.55	0.00001
009 ^{a,b}	382	67	11	0.12	0.41
010	19	0	0		
011	16	0	0		
012 ^a	155	53	39	−0.53	0.00001
013	86	5	9	0.01	0.77
014	2	0	0		
015	22	0	0		
016	17	0	0		
017	23	0	0		
018	8	0	0		
019	3	0	0		
020	4	0	0		
021	17	0	0		
022	84	1	3	0.19	0.003
023	140	24	22	−0.43	0.00001
024	42	0	20	−0.60	0.0001
025	20	0	0		
026	–	–	–		
027	7	0	0		
028	2	0	0		
029	42	0	67	0.29	0.00001
030	50	9	20	−0.38	0.00001
031	19	0	0		
043 ^a	187	79	17	−0.77	0.00001
044 ^a	185	57	4	−0.92	0.00001
045 ^a	205	52	21	−0.45	0.00001
046	13	0	0		
047 ^a	127	50	21	−0.60	0.00001
048 ^{a,b}	175	18	21	0.14	0.13
049 ^{a,b}	102	7	29	0.07	0.08
050 ^a	29	0	59	−0.69	0.00001
051 ^a	62	100	0	0.87	0.00001
065	8	0	0		
066	25	0	49	0.14	0.17
067	24	0	0		
068	3	0	0		
069	36	0	8	0.41	0.00001
070	131	16	7	0.44	0.00001

^a Alluvial aquifer.

^b Different sections of the River Ebro alluvial aquifer.

As a general rule, groundwater flows to areas of lower water table elevation. The analysis of the relationship between nitrate distribution in groundwater and water table elevation (aquifer by aquifer) revealed the existence of advective nitrate transport in the saturated zone (Fig. 4). It was observed that 86% of the alluvial aquifers located in first- and second-order basins (aquifers nos. 012, 043, 044, 045, 047 and 050) showed significant negative correlations between nitrate concentration and water table elevation (Table 3). The results were consistent with the existence of stagnant groundwater zones in the lower sections of these aquifers (Fig. 4), where nitrates tend to accumulate. This provides a good reflection of the key role played by advective transport throughout the alluvial saturated zone. Only one alluvial aquifer (no. 051) showed a significant positive correlation (Table 3), indicating greater pollution in the upper alluvial section (as a result of direct leaching). Alluvial areas nos. 009, 048 and 049 did not reveal any significant correlation. The explanation may lie in the fact that these areas are actually different sections of the Ebro alluvial aquifer (Fig. 4), which do not constitute real hydrogeological units. In these cases, the nitrate contents were controlled by dilution-concentration processes involved in complex hydrological dynamics (since

they receive both polluted and unpolluted waters from a fifth-order basin).

Of the 12 carbonate and detrital sedimentary aquifers affected, or at risk of being affected, by nitrate pollution, six showed significant negative correlations between nitrate concentration and water table elevation (aquifers nos. 002, 003, 008, 023, 024 and 030; Table 3). These results were again consistent with the existence of stagnant zones in the lower sections of the aquifers. In contrast, four carbonate aquifers (nos. 022, 029, 069 and 070) showed significant positive correlations (Table 3), suggesting direct N-leaching from the overlying irrigated and rainfed crops (Fig. 2).

4.2. Intrinsic groundwater vulnerability

The intrinsic groundwater vulnerability map (Fig. 5) reflects the risks associated with natural geological, topographic, hydrological, and climatic attributes, in line with the definition of the IV index. The map showed negligible to low levels of intrinsic vulnerability across 45% of the study area (11,463 km²), moderate levels in 34% (8811 km²) and

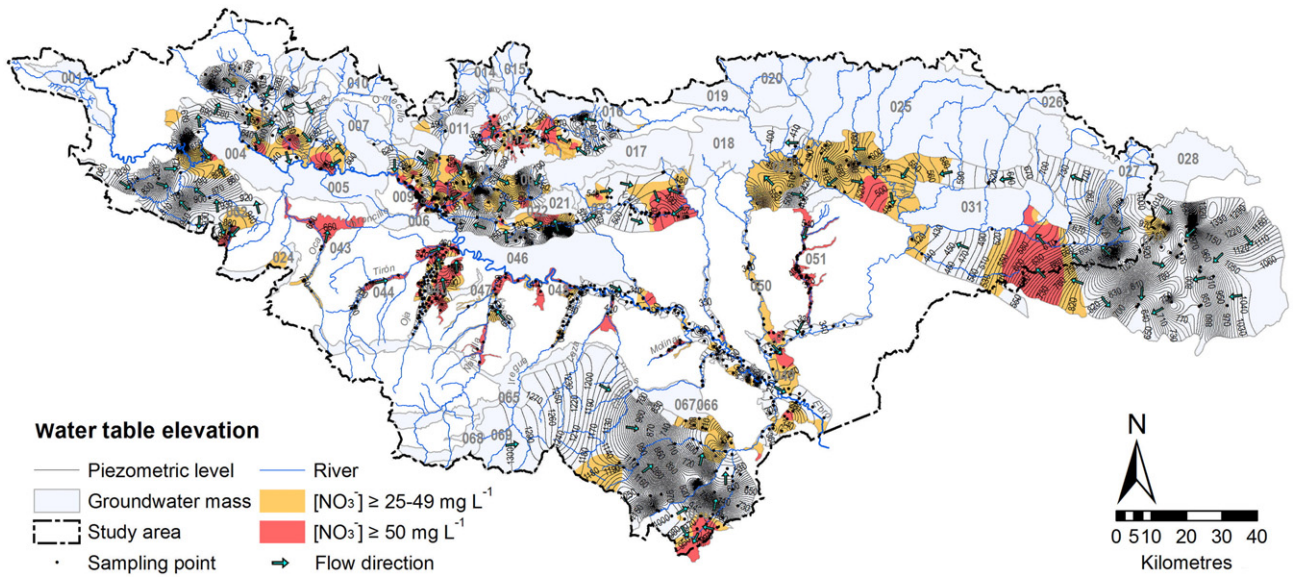


Fig. 4. Water table elevation in aquifers affected and at risk of being affected by nitrate pollution; sampling points used for interpolations and polluted groundwater zones are shown; arrows represent groundwater flow direction.

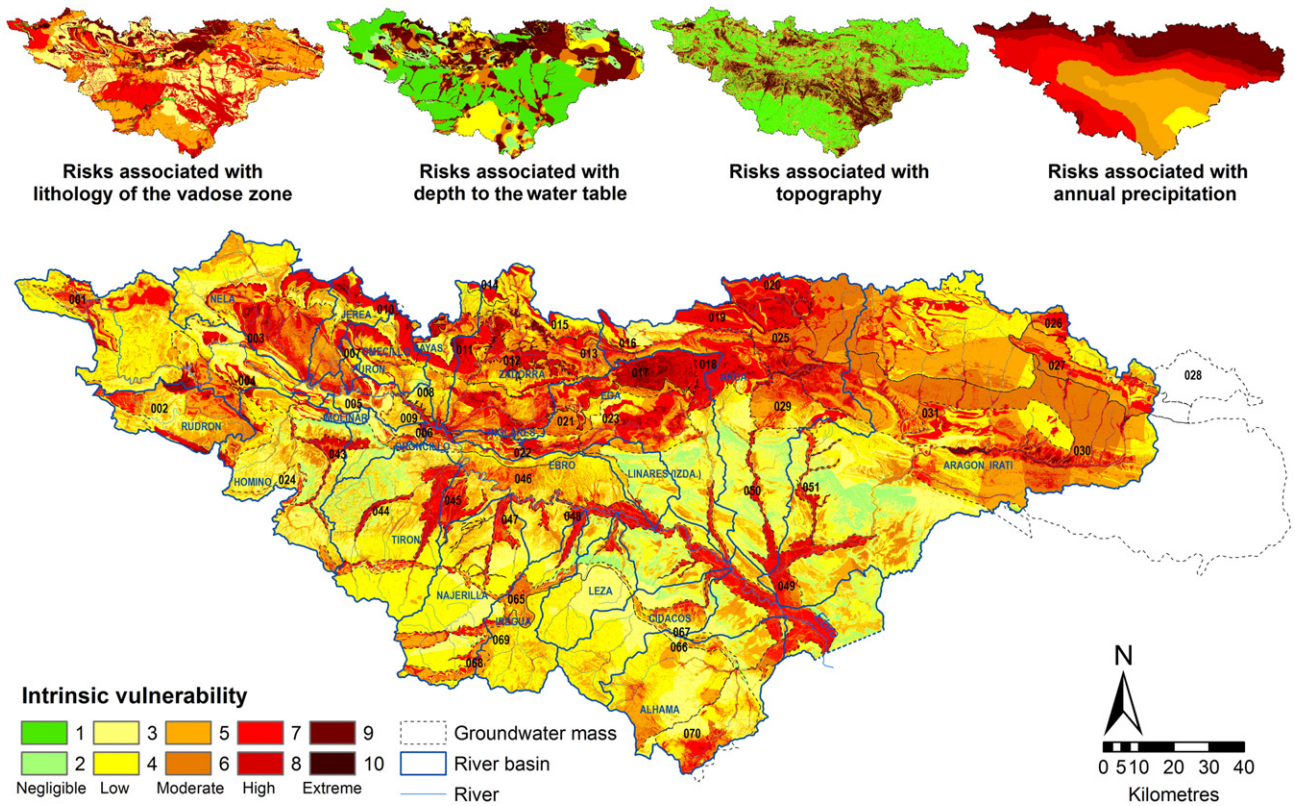


Fig. 5. Intrinsic groundwater vulnerability based on the IV index; maps of the risks associated with the environmental parameters that make up the IV index are shown above.

Table 4

Effective weights from single-parameter sensitivity analysis (W ; Eq. (3)) compared with theoretical weights for the IV index, considering the entire study area; L , D , T and P respectively represent the risks associated with the lithology of the vadose zone, depth of the water table, topography and annual precipitation.

Parameter	Theoretical weight (%)	Effective weight (%)	SD	Minimum (%)	Maximum (%)	n
L	25	26	10	3	66	256,638,138
D	25	20	13	3	75	256,638,138
T	25	18	15	3	75	256,638,138
P	25	36	14	12	100	256,638,138

SD: standard deviation; n: number of values (pixels) used to compute the analysis.

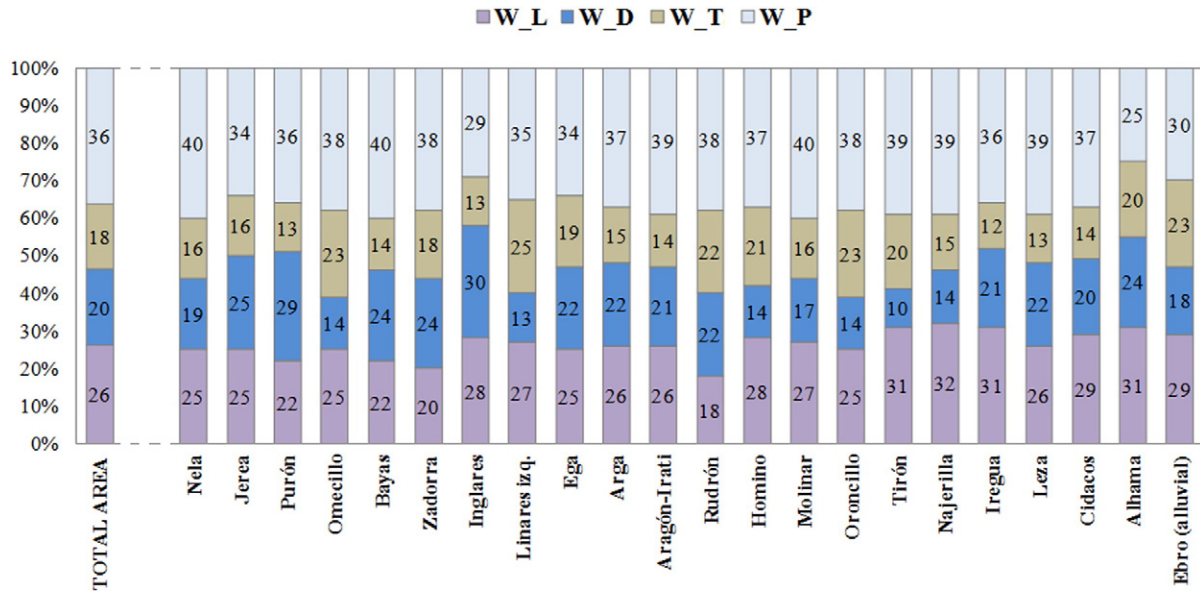


Fig. 6. Effective weights of the four parameters included in the IV index (for the entire study area and for each sub-basin); W_L, W_D, W_T and W_P respectively represent the effective weights of the risks associated with the lithology of the vadose zone, depth of the water table, topography and annual precipitation.

high to extreme levels in 21% (5371 km²). All the alluvial areas were within the range of high to extreme vulnerability. The carbonate aquifers in areas of high precipitation also showed high to extreme degrees of intrinsic vulnerability.

In order to prevent inaccuracies arising as a result of pre-assigning different weights to the input parameters (Hamza et al., 2015), the same

theoretical weight was initially assumed for all four parameters of the IV index. This decision was supported by the results of the single-parameter sensitivity analysis, which was used to compare the theoretical weights assigned to the vulnerability parameters and their effective counterparts under two different ways. The sensitivity analyses for the entire study area showed that the effective weights of parameters P and L

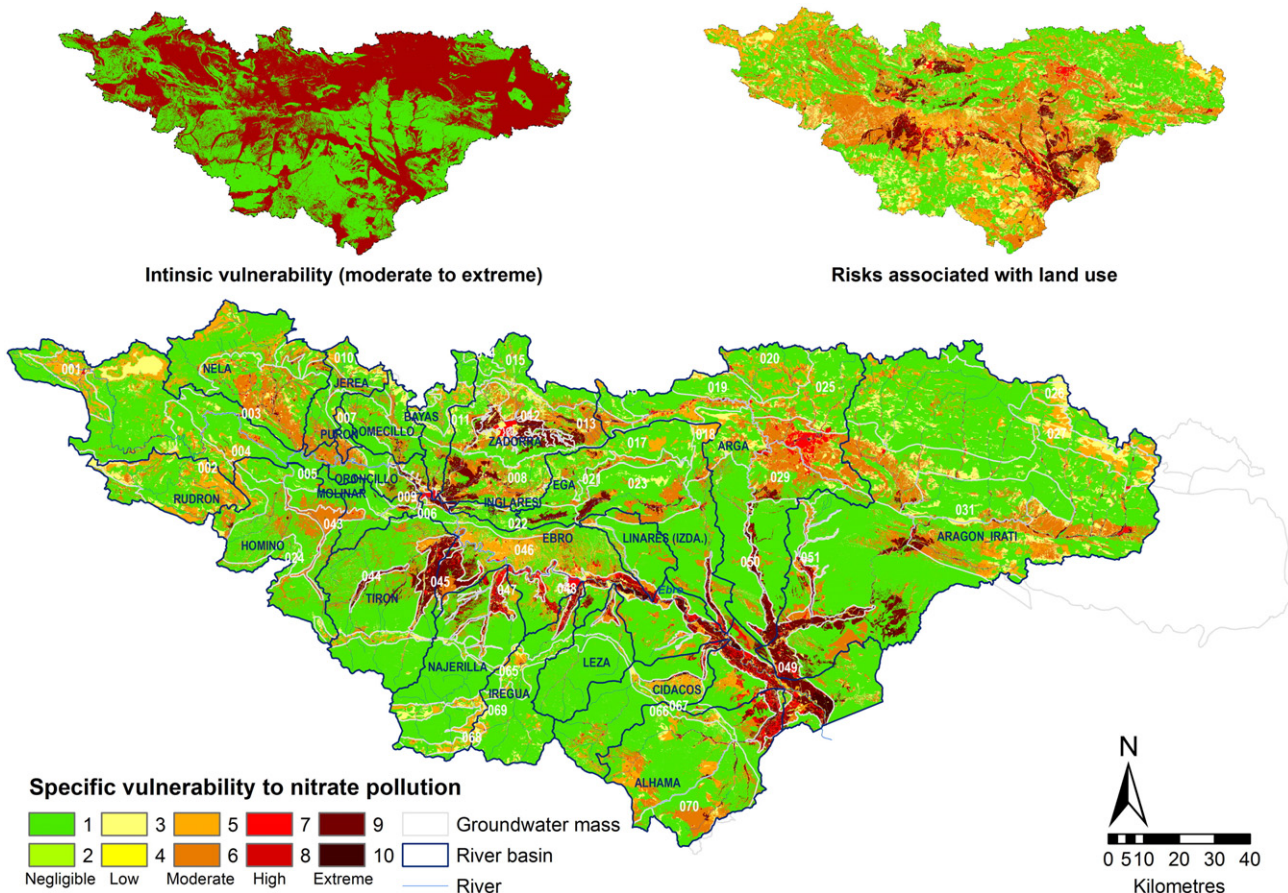


Fig. 7. Specific groundwater vulnerability to nitrate pollution based on the LU-IV procedure; maps of the intrinsic vulnerability 1–0 (moderate to extreme) and the risks associated with land use are shown above.

Table 5

Pearson's correlation (r) between the relative areas of groundwater with high nitrate levels (above 25 mg L⁻¹ and above 50 mg L⁻¹) and the relative areas of NVZ (at moderate-extreme risk and at high-extreme risk), to compare four criteria for groundwater vulnerability, on a basin-by-basin basis. The relative areas were expressed as a percentage of the total area of each basin (%TA). The NVZ were estimated by applying the LU-IV procedure, the IV index, the GOD index and the DRASTIC index. Twenty-one drainage basins were used ($n = 21$). Values in bold: significant correlation at $p \leq 0.05$.

Criteria of vulnerability	NVZ according to the degree of vulnerability	Area of groundwater with NO ₃ ⁻ ≥ 25 mg L ⁻¹ (%TA)		Area of groundwater with NO ₃ ⁻ ≥ 50 mg L ⁻¹ (%TA)	
		r	p-Value	r	p-Value
LU-IV procedure	NVZ moderate-extreme (%TA)	0.64	0.002	0.24	0.29
	NVZ high-extreme (%TA)	0.34	0.13	0.54	0.01
IV index	NVZ moderate-extreme (%TA)	0.55	0.01	0.01	0.96
	NVZ high-extreme (%TA)	0.43	0.05	0.14	0.54
GOD index	NVZ moderate-extreme (%TA)	0.19	0.41	0.01	0.97
	NVZ high-extreme (%TA)	0.12	0.60	0.42	0.06
DRASTIC index	NVZ moderate-extreme (%TA)	0.28	0.22	-0.11	0.63
	NVZ high-extreme (%TA)	0.12	0.60	-0.29	0.20

were slightly greater than their theoretical weights; in contrast, the effective weights of parameters D and T were slightly smaller than these weights (Table 4). What is more, to test whether the weighting system used in generating the vulnerability index was area dependent, or not, additional single-parameter sensitivity analyses were performed for each of the 21 individual river basins in the study area (these were basins with different areas, environmental characteristics and land uses). After analysing this variability on a basin-by-basin basis (Fig. 6) the following ranges of effective weights were found: parameter L from 18 to 32%; parameter D from 10 to 30%; parameter T from 12 to 25%; and parameter P from 25 to 40%. It was, therefore, verified that the size and individual characteristics of the analysis unit (river basin) affected the resulting effective weights (Babiker et al., 2005). To minimize the impact of the subjective component linked to the pre-assignment of different weights on the subsequent output of the model, it was decided to maintain the same theoretical weight for the different parameters that make up the IV index.

Probably, the most novel aspect of the IV index is that it allows us to assess intrinsic vulnerability over the entire topographical surface of the potential catchment area of an aquifer. Although the majority of areas without underlying groundwater were observed to have negligible to low risks of pollution, there were also many enclaves with moderate to high risks that should not be overlooked (Fig. 5). When the vertical infiltration of nitrate takes place in these areas, there is a risk of it being transported through the vadose zone by subsurface runoff (particularly in sloping areas) until it reaches the aquifer. Other advantages of the IV index are that it requires only readily available data and can provide a multi-scale representation in a GIS (the high quality of the input data made it possible to work with a pixel resolution of 10 m).

4.3. Specific groundwater vulnerability to nitrate pollution

The specific groundwater vulnerability map (LU-IV procedure; Fig. 7) reflects the risks associated with land use in territories previously classified as intrinsically vulnerable (Fig. 5). We observed negligible to low levels of vulnerability to nitrate pollution in 73% of the study area (18,738 km²), moderate levels in 20% (5198 km²) and high to extreme levels in the remaining 7% (1728 km²).

It was estimated that 62% of the total alluvial area exhibited high to extreme vulnerability to nitrate pollution, while 24% was subject to moderate risk (Fig. 7). This fact can be explained as a combined effect of several factors (Arauzo et al., 2011) including: the shallow water table in the alluvial aquifers, their interconnections with the surface waters, the permeability of the alluvial deposits and the typically high concentration of irrigated agriculture on the lower terraces and floodplains along river banks (Fig. 2).

On the land above the carbonate and detrital sedimentary aquifers, only 3% of the surface had high to extreme specific vulnerability, while 24% was subject to moderate risk. Likewise, in areas without underlying groundwater, 4% of the surface also exhibited high to extreme

specific vulnerability and 14% moderate risk. In these areas, the risks were associated with irrigated and rainfed agriculture, respectively (Figs. 2 and 7).

Forests and natural areas in mountain headwaters were proven to be non-polluting and protecting land uses, despite their high level of intrinsic vulnerability (Figs. 2, 5 and 7; Martínez-Bastida et al., 2010).

It was easy to define the NVZ based on the map of specific groundwater vulnerability to nitrate pollution (Fig. 7). It was possible to do this by following a restrictive criterion: considering the areas with moderate to extreme specific vulnerability as NVZ (6926 km², 27% of the total area; Table 6). But it would also be possible to use a less restrictive approach: considering the areas with high to extreme specific vulnerability as NVZ (1728 km², 7% of the total area; Table 6). This would only depend on the criteria adopted by the public administrations with competences for designating NVZ. In either case, these results sharply contrast with the current 328 km² (1% of the study area; Fig. 1) officially designated as NVZ by the six Spanish's regional administrations with competencies within the study area.

4.4. Validation of the results

The correlation matrix for the rasters in Fig. 8 revealed significant positive relationships between the five variables at $p \leq 0.01$. The IV index produced a better correlation against the nitrate concentration ($p \leq 0.00001$) than either DRASTIC or GOD. Specific vulnerability based on the LU-IV procedure showed the best correlation ($p \leq 0.00001$). As an initial approximation, this could therefore be regarded as the most reliable of the methods studied.

However, although correlation has been widely used for the validation of vulnerability models (Boy-Roura et al., 2013; Kura et al., 2015; Martínez-Bastida et al., 2010), this still remains a fairly limited approach. This is because a validation based on correlation only considers that aquifers can be recharged by vertical drainage, disregarding the long-distance transportation of solutes from higher to lower areas (Zahid et al., 2015). Basin-scale N-transport processes include: infiltration through the vadose zone (following vertical pathways), surface and subsurface runoff in the vadose zone (when there is a slope), and advective transport through the saturated zone following groundwater flow paths (Arauzo and Martínez-Bastida, 2015). Precipitation is generally the triggering factor for N-transport in rainfed areas, while both precipitation and/or excess irrigation tend to be the triggering factors in irrigated areas (Arauzo and Valladolid, 2013). Bearing this in mind, a more realistic comparison between the four vulnerability models was obtained by calculating Pearson's correlations between the relative areas corresponding to polluted groundwater and the relative areas of NVZ (for each of the four models) on a basin-by-basin basis (Table 5). High significant positive correlations were observed between the relative areas of the NVZ estimated by the LU-IV procedure and the relative areas of groundwater affected by nitrate pollution (NVZ moderate-

Table 6
 Characteristics of the drainage basins in the study area, including: total area (TA); area with groundwater, expressed in km² (GW) and as a percentage of the total area (GW, %TA); aquifers affected and at risk of being affected by nitrate pollution; groundwater areas with nitrate levels above 50 mg L⁻¹ and 25 mg L⁻¹, expressed in km² and as a percentage of the total area of the basin (%TA). NVZ surfaces according to the LU-IV procedure (NVZ at high to extreme risk, NVZ at moderate to extreme risk and zones with negligible to low vulnerability; in km² and as %TA).

River basin (CHE-code)	TA (km ²)	GW (km ²)	GW (%TA)	Aquifers affected and at risk (CHE-code)	NO ₃ ⁻ ≥ 50 mg L ⁻¹ (km ²)	NO ₃ ⁻ ≥ 50 mg L ⁻¹ (%TA)	NO ₃ ⁻ ≥ 25 mg L ⁻¹ (km ²)	NO ₃ ⁻ ≥ 25 mg L ⁻¹ (%TA)	NVZ high-extreme (km ²)	NVZ high-extreme (%TA)	NVZ mod-extreme (km ²)	NVZ mod-extreme (%TA)	No NVZ (km ²)	No NVZ (%TA)
Nela (1)	1086	584	54	003	21	2	81	7	20	2	393	36	693	64
Jerea (3)	309	259	84	003	3	1	28	9	4	1	92	30	217	70
Purón (10)	57	57	100	003	0	0	19	33	0	0	23	40	34	60
Omeçillo (8)	350	322	92	008	0	0	14	4	6	2	67	19	283	81
Bayas (7)	313	312	100	013, 008, 009	11	4	70	22	9	3	65	21	248	79
Zadorra (2)	1356	1356	100	008, 012, 013	147	11	375	28	232	17	566	42	790	58
Inglares (24)	91	91	100	022	2	3	11	12	9	10	18	20	73	80
Linares izq. (5)	308	90	29	048	8	3	14	5	4	1	58	19	250	81
Ega (11)	1522	1089	72	022, 023, 049	126	8	257	17	92	6	377	25	1145	75
Arga (6)	2731	1780	65	029, 030, 050	13	0	117	4	98	4	738	27	1993	73
Aragón-Irati (5, 9, 23)	5864	4152	71	030, 049, 051	357	6	931	16	318	5	1381	24	4483	76
Rudrón (16)	522	466	89	002	0	0	25	5	2	0	181	35	341	65
Homino (17)	1087	407	37	002, 024, 043	69	6	134	12	7	1	304	28	783	72
Molinar (18)	54	54	100	none	0	0	0	0	0	0	5	9	49	91
Oroncillo (21)	228	89	39	009, 043	21	9	21	9	4	2	51	22	177	78
Tirón (26)	1270	220	17	044, 045	68	5	94	7	122	10	320	25	950	75
Najerilla (28)	1105	285	26	045, 047	35	3	52	5	91	8	222	20	883	80
Iregua (30)	663	544	82	048	0	0	7	1	28	4	85	13	578	87
Leza (32)	530	424	80	048	18	3	20	4	8	2	42	8	488	92
Cidacos (37)	696	569	82	069	0	0	41	6	26	4	110	16	586	84
Alhama (38)	1380	1185	86	049, 066, 069, 070	51	4	224	16	114	8	420	30	960	70
Ebro (4) ^a	4139	2073	50	002, 003, 008, 009, 045, 047, 048, 049	166	4	429	10	534	13	1408	34	2731	66
Total study area	25,664	16,411	64		1116	4	2964	12	1728	7	6926	27	18,738	73

^a Ebro (4) includes some alluvial areas of the upper River Ebro and of its minor tributaries; this does not strictly constitute a river basin.

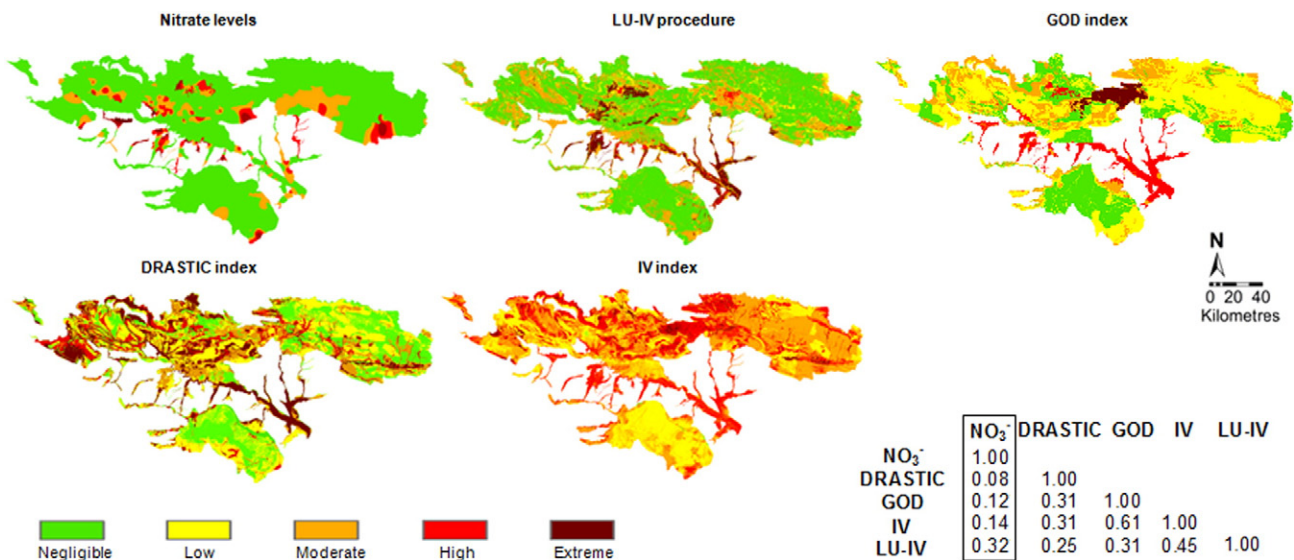


Fig. 8. Rasters of nitrate levels in groundwater, intrinsic vulnerability based on the IV index, intrinsic vulnerability based on the DRASTIC index (IGME, 2009a, 2009b), intrinsic vulnerability based on the GOD index (Arauzo, 2014) and specific vulnerability to nitrate pollution based on the LU-IV procedure; the correlation matrix from the five rasters is shown (number of pixels = 16,411; 16,409 degrees of freedom).

extreme vs. $\text{NO}_3^- \geq 25 \text{ mg L}^{-1}$ and NVZ high-extreme vs. $\text{NO}_3^- \geq 50 \text{ mg L}^{-1}$). A significant positive correlation was also found between the relative areas of the NVZ estimated using the IV index and the relative areas of groundwater with nitrate levels above 25 mg L^{-1} . The other indexes did not show any significant correlation. These results confirmed the high level of reliability of the LU-IV procedure for assessing and mapping groundwater vulnerability to nitrate pollution.

The basin-by-basin assessment (Table 6) revealed great variability across basins with regard to the size of the NVZ (based on the LU-IV procedure) and to subsequent influences on nitrate distribution in groundwater. The NVZ at high to extreme risk represented 0–17% of the area of the basins. Taking a more conservative approach, the NVZ at moderate to extreme risk covered 8–42% of the basins (Table 6).

5. Conclusions

The LU-IV procedure proposed for assessing and mapping groundwater vulnerability to nitrate pollution has proven to be more effective than the currently most widely-used and accepted methods (DRASTIC and GOD). This novel tool stands out as it meets the following requirements: (1) it uses readily available parameters that provide enough data to feed the model, (2) it excludes redundant parameters, (3) it avoids the need to assign insufficiently contrasted weights to parameters, (4) it assesses the entire catchment area that potentially drains N-polluted waters into the receptor aquifer, (5) it is implementable within a GIS, and (6) it provides a multi-scale representation.

The LU-IV procedure provides a new, reliable tool for delimiting NVZ. It would be particularly interesting to use it in countries (including Spain) in which there is only limited, or even no, access to certain types of environmental data.

The specific groundwater vulnerability map (based on the LU-IV procedure) showed negligible to low levels of vulnerability to nitrate pollution in 73% of the study area, moderate levels in 20% and high to extreme levels in the remaining 7%. From these findings it was concluded that at least an area of 1728 km^2 should be considered as NVZ. This contrasts sharply with the current 328 km^2 officially designated in the upper basin of the River Ebro by the Spain's regional administrations with competencies for designating NVZ. These results highlight the need to redefine what have been the officially designed NVZ in the study area until now. In other words, if we want to effectively implement action programmes designed to restore and protect water quality, in line with Directive 91/676/EEC, it is first necessary to review the current criteria for the designation of NVZ.

Acknowledgements

This work was supported by the Spain's Ministry of Science and Innovation (Project AGL2011-29861). The Ebro Hydrographic Confederation, the Geological and Mining Institute of Spain and the Basque Water Agency supplied hydrochemical and hydrological data. The Spanish Ministry of Agriculture, Food and the Environment provided the digital version of the Crops and Land Use map of Spain (2000–2009). The Ebro Hydrographic Confederation provided the digital version of the Geological map of the River Ebro basin (MAGNA Series, produced by the Spanish Geological Institute).

References

- Allen, R.G., Pereira, L.A., Raes, D., Smith, M., 1998. *Crop evapotranspiration (guidelines for computing crop water requirements)*. FAO Irrigation and Drainage, Paper n° 56, Rome.
- Aller, L., Bennet, T., Lehr, J.H., Petty, R.J., 1987. DRASTIC. A standardized system for evaluating groundwater pollution potential using hydrogeologic settings. U.S. EPA Report 600/2-87-035, Oklahoma.
- Anjali, S., Srivastav, S.K., Kumar, S., Chakrapani, G.J., 2015. A modified-DRASTIC model (DRASTICA) for assessment of groundwater vulnerability to pollution in an urbanized environment in Lucknow, India. *Environ. Earth Sci.* 74, 5475–5490.
- Arauzo, M., 2014. Groundwater vulnerability to nitrate pollution in the upper River Ebro basin: GOD index ad risks associated with land use (Vulnerabilidad de las aguas subterráneas a la contaminación por nitrato en la Cuenca Alta del Ebro: índice GOD y riesgos asociados a los usos del territorio; Spanish). In: Gómez-Hernández, J.J., Rodrigo-Illari, J. (Eds.), *II Congreso Ibérico de las Aguas Subterráneas: CIAS 2014 Valencia*. Editorial Universitat Politècnica de València, Valencia, pp. 33–54.
- Arauzo, M., Martínez-Bastida, J.J., 2015. Environmental factors affecting diffuse nitrate pollution in the major aquifers of central Spain: groundwater vulnerability vs. groundwater pollution. *Environ. Earth Sci.* 73, 8272–8286.
- Arauzo, M., Valladolid, M., 2013. Drainage and N-leaching in alluvial soils under agricultural land uses: implications for the implementation of the EU Nitrates Directive. *Agric. Ecosyst. Environ.* 179, 94–107.
- Arauzo, M., Martínez-Bastida, J.J., Valladolid, M., Díez, J.A., 2010. Field evaluation of Gee Passive Capillary Lysimeters for monitoring drainage in non-gravelly and gravelly alluvial soils: A useful tool to estimate nitrogen leaching from agriculture. *Agric. Water Manage.* 97, 465–474.
- Arauzo, M., Valladolid, M., Martínez-Bastida, J.J., 2011. Spatio-temporal dynamics of nitrogen in river-alluvial aquifer systems affected by diffuse pollution from agricultural sources: implications for the implementation of the Nitrate Directive. *J. Hydrol.* 411, 155–168.
- Babiker, I.S., Mohamed, M.A., Hiyama, T., Kato, K., 2005. A GIS-based DRASTIC model for assessing aquifer vulnerability in Kakamigahara Heights, Gifu Prefecture, central Japan. *Sci. Total Environ.* 345, 127–140.
- Botey, R., Guijarro, J.A., Jiménez, A., 2013. Normal monthly precipitation from 1981–2010 (Valores normales de precipitación mensual 1981–2010; Spanish). Dirección de Producción e Infraestructuras. Agencia Estatal de Meteorología (AEMET), Ministerio de Agricultura, Alimentación y Medio Ambiente, Madrid.
- Boy-Roura, M., Nolan, B.T., Menció, A., Mas-Pla, J., 2013. Regression model for aquifer vulnerability assessment of nitrate pollution in the Osona region (NE Spain). *J. Hydrol.* 505, 150–162.
- CHE, 2015. GeoPortal Sitebro. Geodata. Retrieved from <http://iber.chebro.es/geoportal/>.
- Council of the European Communities, 1991. Directive 91/676/EEC Concerning the Protection of Waters Against Pollution Caused by Nitrates From Agricultural Sources. 12 December 1991. Council of the European Communities, Brussels.
- De Clercq, P., Gertsis, A.C., Hofman, G., Jarvis, S.C., Neeteson, J.J., Sinabell, F. (Eds.), 2001. *Nutrient Management Legislation in European Countries*. Ghent University, Department of Soil Management and Soil Care, Ghent.
- Debernardi, L., De Luca, D.A., Lasagna, M., 2012. Correlation between nitrate concentration in groundwater and parameters affecting aquifer intrinsic vulnerability. *Environ. Geol.* 55, 539–558.
- Dixon, B., 2005. Groundwater vulnerability mapping: a GIS and fuzzy rule based integrated tool. *Appl. Geogr.* 25, 327–347.
- ESRI, 2011. ArcGIS Desktop: Release 10. Environmental Systems Research Institute, Redlands, California.
- European Commission, 2000. Nitrates Directive (91/676/EEC). Status and Trends of Aquatic Environment and Agricultural Practice. Development Guide for Member States' Reports. Directorate-General for Environment, Brussels.
- European Commission, 2010. On Implementation of Council Directive 91/676/EEC Concerning the Protection of Waters Against Pollution Caused by Nitrates From Agricultural Sources Based on Member State Reports for the Period 2004–2007. Commission Staff Working Document, Brussels.
- Foster, S.S.D., 1987. Fundamental concepts in aquifer vulnerability, pollution risk and protection strategy. In: van Duijvanbooden, W., van Waegeningh, H.G. (Eds.), *Vulnerability of Soil and Groundwater to Pollution Proceedings and Information No. 38*. TNO Committee on Hydrological Research, the Netherlands.
- Foster, S., 2007. Aquifer pollution vulnerability concept and tools-use, benefits and constraints. In: Witkowski, A., Kowalczyk, A., Vrba, J. (Eds.), *Groundwater Vulnerability Assessment and Mapping International Association of Hydrogeologists Selected Papers vol. 11*. Taylor & Francis, London.
- Foster, S., Hirata, R., Gómez, D., D'Elia, M., Paris, M., 2002. *Ground Water Quality Protection. A Guide for Water Utilities, Municipal Authorities and Environment Agencies*. The World Bank, Washington D.C.
- Hamza, S.M., Ahsan, A., Imteaz, M.A., Rahman, A., Mohammad, T.A., Ghazali, A.H., 2015. Accomplishment and subjectivity of GIS-based DRASTIC groundwater vulnerability assessment method: a review. *Environ. Earth Sci.* 73, 3063–3076.
- Holman, I.P., Palmer, R.C., Bellamy, P.H., Hollis, J.M., 2005. Validation of an intrinsic groundwater pollution vulnerability methodology using a national nitrate database. *Hydrogeol. J.* 13, 665–674.
- Huan, H., Wang, J., Teng, Y., 2012. Assessment and validation of groundwater vulnerability to nitrate based on a modified DRASTIC model: a case study in Jilin City of northeast China. *Sci. Total Environ.* 440, 14–23.
- IBM Corp., 2014. *IBM SPSS Statistics for Windows, Version 23.0*. IBM Corp., Armonk, NY.
- IGME, 2009a. Map of Groundwater Vulnerability to Pollution. Reduced Version of the DRASTIC Index. Ebro River Basin. Assessment of the Intrinsic Vulnerability of Intercommunity Groundwater. Detritic and Mixed Masses (Mapa de vulnerabilidad a la contaminación del agua subterránea. Índice DRASTIC reducido. Demarcación Hidrográfica del Ebro. Evaluación de la vulnerabilidad intrínseca de las aguas subterráneas intercomunitarias. Masas detriticas y mixtas; Spanish) [Map in Digital Format]. 1:1,000,000. Instituto Geológico y Minero de España, Dirección General del Agua Retrieved from <http://www.igme.es/>.
- IGME, 2009b. Map of Groundwater Vulnerability to Pollution. Reduced Version of the DRASTIC Index. Ebro River Basin. Assessment of the Intrinsic Vulnerability of Intercommunity Groundwater. Carbonated Masses (Mapa de vulnerabilidad a la contaminación del agua subterránea. Índice DRASTIC reducido. Demarcación Hidrográfica del Ebro. Evaluación de la vulnerabilidad intrínseca de las aguas subterráneas intercomunitarias. Masas carbonatadas; Spanish) [Map in Digital

- Format]. 1:1,000,000. Instituto Geológico y Minero de España, Dirección General del Agua Retrieved from <http://www.igme.es/>.
- Javadi, S., Kavehkar, N., Mohammadi, K., Khodadadi, A., Kahawita, R., 2011. Calibrating DRASTIC using field measurements, sensitivity analysis and statistical methods to assess groundwater vulnerability. *Water Int.* 36, 719–732.
- Kura, N.U., Ramli, M.F., Ibrahim, S., Sulaiman, W.N.A., Aris, A.Z., Tanko, A.I., Zaudi, M.A., 2015. Assessment of groundwater vulnerability to anthropogenic pollution and seawater intrusion in a small tropical island using index-based methods. *Environ. Sci. Pollut. Res.* 22, 1512–1533.
- Lubianetzky, T.A., Dickson, S.E., Guo, Y., 2015. Proposed method: incorporation of fractured rock in aquifer vulnerability assessments. *Environ. Earth Sci.* 74, 4813–4825.
- MAGRAMA, 2005. Characterization of Groundwater Masses in Intercommunity Basins. Volume V (Caracterización de las masas de agua subterránea de las cuencas intercomunitarias. Tomo V; Spanish). Ministerio de Agricultura, Alimentación y Medio Ambiente, Madrid.
- MARM, 2009. Crops and Land Use Map of Spain 2000–2009 (Mapa de Cultivos y Aprovechamientos de España 2000–2009; Spanish) [Maps in Digital Format]. 1: 50,000. Ministerio de Agricultura y del Medio Rural y Marino, Madrid.
- Martínez-Bastida, J.J., Arauzo, M., Valladolid, M., 2010. Intrinsic and specific vulnerability of groundwater in Central Spain: the risk of nitrate pollution. *Hydrogeol. J.* 18, 681–698.
- Menció, A., Mas-Pla, J., Otero, N., Regàs, O., Boy-Roura, M., Puig, R., Bach, J., Domènech, C., Zamorano, M., Brusi, D., Folch, A., 2016. Nitrate pollution of groundwater; all right... but nothing else? *Sci. Total Environ.* 539, 241–251.
- Neshat, A., Pradhan, B., 2015. An integrated DRASTIC model using frequency ratio and two new hybrid methods for groundwater vulnerability assessment. *Nat. Hazards* 76, 543–563.
- Secunda, S., Collin, M.L., Melloul, A.J., 1998. Groundwater vulnerability assessment using a composite model combining DRASTIC with extensive agricultural land use in Israel's Sharon region. *J. Environ. Manag.* 54, 39–57.
- Shirazi, S.M., Imran, H.M., Akib, S., 2012. GIS-based DRASTIC method for groundwater vulnerability assessment: a review. *J. Risk Res.* 15, 991–1011.
- Stigter, T.Y., Ribeiro, L., Carvalho Dill, A.M.M., 2006. Evaluation of an intrinsic and a specific vulnerability assessment method in comparison with groundwater salinisation and nitrate contamination levels in two agricultural regions in the south of Portugal. *Hydrogeol. J.* 14, 79–99.
- Sutton, M.A., Howard, C.M., Erisman, J.W., Billen, G., Bleeker, A., Grennfelt, P., van Grisven, H., Grizzetti, B., 2011. *The European Nitrogen Assessment: Sources, Effects and Policy Perspectives*. Cambridge University Press, Cambridge.
- Wachniew, P., Zurek, A.J., Stumpp, C., Gemtzi, A., Gargini, A., Filippini, M., Rozanski, K., Meeks, J., Kvaerner, J., Witczak, S., 2016. Towards operational methods for the assessment of intrinsic groundwater vulnerability: a review. *Crit. Rev. Environ. Sci. Technol.* 46, 827–884.
- Witkowski, A., Kowalczyk, A., Vrba, J. (Eds.), 2007. *Groundwater vulnerability assessment and mapping* International Association of Hydrogeologists Selected Papers vol. 11. Taylor & Francis, London.
- Worrall, F., Spencer, E., Burt, T.P., 2009. The effectiveness of nitrate vulnerable zones for limiting surface water nitrate concentrations. *J. Hydrol.* 370, 21–28.
- Zahid, A., Hassan, M.Q., Ahmed, K.M.U., 2015. Simulation of flowpaths and travel time of groundwater through arsenic-contaminated zone in the multi-layered aquifer system of Bengal Basin. *Environ. Earth Sci.* 73, 979–991.